HOME

Spacecraft Formation Flying near Sun-Earth L_2 Lagrange Point: Trajectory Generation and Adaptive Full-State Feedback Control

Hong Wong and Vikram Kapila
Department of Mechanical, Aerospace, and Manufacturing Engineering
Polytechnic University, Brooklyn, NY 11201
[hwong01@utopia, vkapila@duke].poly.edu

In this paper, we present a method for trajectory generation and adaptive full-state feedback control to facilitate spacecraft formation flying near the Sun-Earth L_2 Lagrange point. Specifically, the dynamics of a spacecraft in the neighborhood of a Halo orbit reveals that there exist quasi-periodic orbits surrounding the Halo orbit. Thus, a spacecraft formation is created by placing a leader spacecraft on a desired Halo orbit and placing follower spacecraft on desired quasi-periodic orbits. To produce a formation maintenance controller, we first develop the nonlinear dynamics of a follower spacecraft relative to the leader spacecraft. We assume that the leader spacecraft is on a desired Halo orbit trajectory and the follower spacecraft is to track a desired quasi-periodic orbit surrounding the Halo orbit. Then, we design an adaptive, full-state feedback position tracking controller for the follower spacecraft providing an adaptive compensation for the unknown mass of the follower spacecraft. The proposed control law is simulated for the case of the leader and follower spacecraft pair and is shown to yield global, asymptotic convergence of the relative position tracking errors.

I. Introduction

The Lagrange points of the Sun-Earth system have been exploited as key locations for space-based astronomical observation stations.[1,2] These locations are equilibrium positions in the restricted three body problem (RTBP), see Figure 1(a) for details. The first three Lagrange points in the RTBP (labeled as L_1, L_2, and L_3) are points that are collinear with the two primary masses (Sun and Earth). The last two Lagrange points in the RTBP (labeled as L_4 and L_5) are equilibrium points such that each of these points combined with the two primary masses yields an equilateral triangle. Each of the five equilibrium positions can host a spacecraft for an indefinite time period. A benefit of using a Lagrange point observation station is that spacecraft near these points obtain nearly an unobstructed view of the galaxy. Furthermore, missions near the Lagrange points are sufficiently far from the Earth, such that environmental effects (e.g., atmospheric and geomagnetic forces) do not affect spacecraft dynamics.

Future space missions,[3] that intend to utilize the L_2 Lagrange point as the location for deep-space observations and/or interstellar communication have the advantage that solar influences on the spacecraft are minimal and space observations can be conducted on a frequent basis. In contrast, spacecraft that are to perform the same types of missions in either Sun-synchronous or low Earth orbits about the Earth are not suitable because these orbits expose the spacecraft to harsh physical conditions (e.g., gravitational and/or atmospheric disturbances, space debris, etc.).

Recently, the European Space Agency has proposed the Darwin space mission,[4] which is to be deployed near the L_2 Lagrange point where it will search for life in the universe and investigate the evolution of

galaxies. Scheduled for launch in 2014, the Darwin space mission will utilize six spacecraft to cooperatively work together in order to search nearby planets for traces of life, in the form of infrared radiation.

An emerging technology to enhance space-based imaging/interferometry missions is spacecraft formation flying (SFF). SFF enhances space mission performance by distributing mission tasks, which are usually conducted by a monolithic spacecraft, to many small spacecraft. Thus, future space missions near the Sun-Earth Lagrange points can greatly benefit from SFF. However, to effectively utilize this new technology for space missions near the Sun-Earth Lagrange points requires proper design of spacecraft formations and for each spacecraft in the formation to be precisely controlled to maintain a meaningful baseline.

Current spacecraft trajectory designs near the Sun-Earth Lagrange points consist of computing periodic trajectories in the form of Lyapunov and Halo orbits around a Lagrange point.[5–7] Unfortunately, these designs are used specifically to provide desired reference trajectories only for single spacecraft missions. In the current literature for SFF near a Lagrange point, a *leader* spacecraft is placed on a periodic orbit, e.g., a Halo orbit, around a Sun-Earth Lagrange point and a *follower* spacecraft is placed near this periodic orbit and a reference trajectory of the follower spacecraft relative to the leader spacecraft is designed. In Ref. 8, reference trajectories for follower spacecraft are computed using classical orbital elements, which result in bounded orbits around the leader spacecraft on a periodic orbit. In Ref. 9, feedback control is utilized to produce reference trajectories for follower spacecraft. In addition, Ref. 10 provides a method of generating reference trajectories for follower spacecraft using a numerical method, where the resulting trajectories are quasi-periodic.

In this paper, we develop a leader-follower spacecraft formation, where the leader spacecraft is on a periodic, Halo orbit around the L_2 Lagrange point in the Sun-Earth system and the follower spacecraft is to track a desired relative trajectory. Specifically, we first develop the dynamics of the follower spacecraft relative to the leader spacecraft. Next, in the spirit of Ref. 10, we design a desired quasi-periodic relative trajectory for the follower spacecraft. In contrast to Ref. 10, our trajectory design exploits the analytical properties of the quasi-periodic relative trajectories to characterize spacecraft formations using a set of parameters. Finally, we develop an adaptive full-state feedback control algorithm to enable the follower spacecraft to track this desired quasi-periodic relative trajectory.

This paper is organized as follows. Section II develops the mathematical model for the follower spacecraft relative to the leader spacecraft. Section III describes a method of generating follower spacecraft trajectories relative to the leader spacecraft orbit to create a spacecraft formation. Section IV formulates a trajectory tracking control problem. Section V uses a Lyapunov-based approach to design a full-state feedback control law and a parameter update algorithm, which facilitate the tracking of given reference trajectories in the presence of unknown follower spacecraft mass. Illustrative simulations are included in Section VI to demonstrate the efficacy of the proposed trajectory generation and control design schemes. Finally, some concluding remarks are given in Section VII.

II. System Model

In this section, we develop a nonlinear model characterizing the position dynamics of the follower spacecraft relative to the leader spacecraft near the L_2 Lagrange point in the Sun-Earth system. Referring to Figure 1, we assume that the Earth and the Sun rotate in a circular orbit around the Sun-Earth system barycenter (center of mass) with a constant angular speed ω. In addition, we attach an inertial coordinate system $\{X, Y, Z\}$ to the Sun-Earth system barycenter and a rotating, right-handed coordinate frame $\{x_{L_2}, y_{L_2}, z_{L_2}\}$ to the L_2 Lagrange point with the x_{L_2}-axis pointing along the direction from the Sun to the Earth, the z_{L_2}-axis pointing along the orbital angular momentum of the Sun-Earth system, and the y_{L_2}-axis being mutually perpendicular to the x_{L_2} and z_{L_2} axes, and pointing in the direction that completes the right-handed coordinate frame.

A. Dynamics of a Spacecraft Relative to the L_2 Lagrange Point

In order to describe the dynamics of a spacecraft formation near the L_2 Lagrange point, we must first describe the dynamics of a spacecraft relative to the L_2 Lagrange point. To do so, let $q(t) \triangleq [x \quad y \quad z]^T \in \mathbb{R}^3$ denote the position vector from the spacecraft to the L_2 Lagrange point, expressed in the $\{x_{L_2}, y_{L_2}, z_{L_2}\}$ coordinate frame. In addition, let $R_{S\to s}(t) \in \mathbb{R}^3$ and $R_{E\to s}(t) \in \mathbb{R}^3$ denote the position vectors from the Sun and Earth, respectively, to the spacecraft. Finally, let R_{L_2}, R_E, and R_S denote the distances between the Sun-Earth system barycenter and the L_2 Lagrange point, the Earth, and the Sun, respectively. Then, the mathematical model describing the position of a spacecraft relative to the L_2 Lagrange point is given by[11]

$$m\ddot{q} + C\dot{q} + N(q, s) = u, \tag{1}$$

where m is the mass of the spacecraft, C is a Coriolis-like matrix defined as $C \triangleq 2m\omega \begin{bmatrix} 0 & -1 & 0 \\ 1 & 0 & 0 \\ 0 & 0 & 0 \end{bmatrix}$, N is a nonlinear term consisting of gravitational effects and inertial forces

$$N \triangleq m \begin{bmatrix} \frac{\mu_S(x+R_{L_2}+R_S)}{\|R_{S\to s}\|^3} + \frac{\mu_E(x+R_{L_2}-R_E)}{\|R_{E\to s}\|^3} - \omega^2(x+R_{L_2}) \\ \frac{\mu_S\, y}{\|R_{S\to s}\|^3} + \frac{\mu_E\, y}{\|R_{E\to s}\|^3} - \omega^2 y \\ \frac{\mu_S\, z}{\|R_{S\to s}\|^3} + \frac{\mu_E\, z}{\|R_{E\to s}\|^3} \end{bmatrix},$$

and $u(t) \in \mathbb{R}^3$ is the thrust control input to the spacecraft. Furthermore, the constants μ_E and μ_S in the definition of N are defined as $\mu_E \triangleq GM_E$ and $\mu_S \triangleq GM_S$, respectively, where G is the universal gravitational constant, M_E is the mass of the Earth, and M_S is the mass of the Sun.

B. Halo Orbit Trajectory

In this subsection, we describe a method to generate thrust-free, periodic trajectories around the L_2 Lagrange point in the form of Halo orbits. We present a succinct overview of a numerical algorithm to generate these periodic trajectories. Additional details on the generation of these periodic trajectories can be found in Refs. 5–7.

One numerical method[7] of generating thrust-free periodic orbits around the L_2 Lagrange point in the Sun-Earth system involves finding a proper set of position and velocity initial conditions to propagate the spacecraft dynamics of (1), with the control thrust u set to zero. First, the Poincaré-Lindstedt method is used to find a high order analytic approximation to a periodic trajectory in the neighborhood of the L_2 Lagrange point. Next, the initial conditions, based on the Poincaré-Lindstedt method, are used as an initial seed in a numerical algorithm to find a better set of initial conditions leading to a periodic trajectory. This numerical algorithm applies a Taylor series expansion to the spacecraft states with respect to the initial conditions and time and truncates higher order terms, such that for Halo orbits the result is a set of 3 linear equations with 4 unknown variables. Families of orbits can be characterized by fixing one of the unknown variables so that the result gives an equal number of equations to unknowns. Solving the aforementioned linear matrix equation and using the result to update the previous set of initial conditions provide a new initial condition guess.

The spacecraft dynamics are then propagated using the new updated set of initial conditions to verify trajectory periodicity. If the trajectory is sufficiently close to being periodic, then the initial conditions can be used for further simulation, else the above numerical algorithm is used to solve for a new set of initial conditions. Since the collinear Lagrange points are inherently unstable,[7] long-term propagation of spacecraft dynamics using the initial conditions obtained in the above manner is futile. However, by exploiting the symmetry property of Halo orbits (see below), we can artificially obtain a periodic orbit by computing trajectory information during half of a period and reusing this trajectory data throughout other simulations.

Halo orbits are classified as periodic trajectories that are symmetric with respect to the $\{x_{\mathrm{L}_2}, z_{\mathrm{L}_2}\}$ plane (i.e., $y_{\mathrm{L}_2} = 0$), and are not confined to be in the orbital plane of the Sun and Earth. Halo orbits have the distinguishing characteristic that their projections on the $\{y_{\mathrm{L}_2}, z_{\mathrm{L}_2}\}$ plane are curves that resemble a Halo. In this paper, we let $q_{\mathrm{H}}(t) = [x_{\mathrm{H}}(t)\ y_{\mathrm{H}}(t)\ z_{\mathrm{H}}(t)]^T \in \mathbb{R}^3$ denote the position vector from a point on a Halo orbit to the L_2 Lagrange point, expressed in the $\{x_{\mathrm{L}_2}, y_{\mathrm{L}_2}, z_{\mathrm{L}_2}\}$ coordinate frame. An initial seed for the numerical algorithm of Ref. 7 consists of a spacecraft starting on the $\{x_{\mathrm{L}_2}, z_{\mathrm{L}_2}\}$ plane with a nonzero initial y_{L_2} and z_{L_2} velocity (i.e., $q_{\mathrm{H}}(0) = [x_{\mathrm{H}}(0) \quad 0 \quad z_{\mathrm{H}}(0)]^T$ and $\dot{q}_{\mathrm{H}}(0) = [0 \quad \dot{y}_{\mathrm{H}}(0) \quad \dot{z}_{\mathrm{d}}(0)]^T$). Updates to the initial x_{L_2} position and y_{L_2} velocity contribute to finding a closed periodic trajectory. In addition, the initial z_{L_2} position determines the size of the Halo orbit. Figure 1(b) shows a typical Halo orbit trajectory around the L_2 Lagrange point.

In this paper, we use Halo orbits as the reference trajectory for the leader spacecraft. The control design framework of Ref. 11 can be employed to ensure that the spacecraft dynamics of (1) tracks a Halo orbit reference trajectory. In a subsequent subsection, we will describe the dynamics of the follower spacecraft relative to the leader spacecraft on the Halo orbit. Finally, we denote $R_{\mathrm{S}\to\mathrm{H}}(t) \in \mathbb{R}^3$ and $R_{\mathrm{E}\to\mathrm{H}}(t) \in \mathbb{R}^3$ as the position vectors from the Sun and the Earth, respectively, to the Halo orbit.

Remark II.1 *The Halo orbit trajectory satisfies the spacecraft dynamics of (1) under the condition that the spacecraft control input is zero. Moreover, we express the leader spacecraft dynamics on the Halo orbit as*

$$m\ddot{q}_{\mathrm{H}} + C\dot{q}_{\mathrm{H}} + N(q_{\mathrm{H}}, \mathrm{H}) = 0. \tag{2}$$

We note that the Halo orbit is a periodic trajectory with a frequency denoted as ω_{H}.

C. Follower Spacecraft Dynamics

In this subsection, we describe the dynamics of the follower spacecraft relative to the leader spacecraft tracking a no-thrust, periodic Halo orbit trajectory q_{H} without deviating from this orbit for all time. To describe the dynamics of the follower spacecraft, we express the position vector of the follower spacecraft relative to the L_2 Lagrange point in the coordinate frame $\{x_{\mathrm{L}_2}, y_{\mathrm{L}_2}, z_{\mathrm{L}_2}\}$ as $q_{\mathrm{f}_{\mathrm{L}_2}}(t) = \begin{bmatrix} x_{\mathrm{f}_{\mathrm{L}_2}} & y_{\mathrm{f}_{\mathrm{L}_2}} & z_{\mathrm{f}_{\mathrm{L}_2}} \end{bmatrix}^T \in \mathbb{R}^3$. In addition, we denote $R_{\mathrm{S}\to\mathrm{s_f}}(t) \in \mathbb{R}^3$ and $R_{\mathrm{E}\to\mathrm{s_f}}(t) \in \mathbb{R}^3$ as the position vectors from the Sun and Earth, respectively, to the follower spacecraft. Using (1), the follower spacecraft dynamics relative to the L_2 Lagrange point can be expressed as

$$m_{\mathrm{f}}\ddot{q}_{\mathrm{f}_{\mathrm{L}_2}} + C_{\mathrm{f}}\dot{q}_{\mathrm{f}_{\mathrm{L}_2}} + N_{\mathrm{f}_{\mathrm{L}_2}}(q_{\mathrm{f}_{\mathrm{L}_2}}, \mathrm{s_f}) = u_{\mathrm{f}}, \tag{3}$$

where m_{f} is the mass of the follower spacecraft, C_{f} is a Coriolis-like matrix defined as $C_{\mathrm{f}} \triangleq 2m_{\mathrm{f}}\omega \begin{bmatrix} 0 & -1 & 0 \\ 1 & 0 & 0 \\ 0 & 0 & 0 \end{bmatrix}$, $N_{\mathrm{f}_{\mathrm{L}_2}}$ is a nonlinear term consisting of gravitational effects and inertial forces defined as $N_{\mathrm{f}_{\mathrm{L}_2}} \triangleq \frac{m_{\mathrm{f}}}{m} N(q_{\mathrm{f}_{\mathrm{L}_2}}, \mathrm{s_f})$, and $u_{\mathrm{f}}(t) \in \mathbb{R}^3$ is the thrust control input to the follower spacecraft.

Next, we define the relative position between the follower and the leader spacecraft $q_{\mathrm{f}}(t) \in \mathbb{R}^3$ as $q_{\mathrm{f}} \triangleq q_{\mathrm{f}_{\mathrm{L}_2}} - q_{\mathrm{H}}$. To obtain the dynamics of the follower spacecraft relative to the leader spacecraft, we differentiate q_{f} with respect to time twice and multiply both sides of the resulting equation by m_{f} to produce

$$m_{\mathrm{f}}\ddot{q}_{\mathrm{f}} = m_{\mathrm{f}}\ddot{q}_{\mathrm{f}_{\mathrm{L}_2}} - m_{\mathrm{f}}\ddot{q}_{\mathrm{H}}. \tag{4}$$

Next, we solve for $\ddot{q}_{\mathrm{H}}$ in (2), multiply the resulting equation by m_{f}, and substitute the result into (4) to yield

$$m_{\mathrm{f}}\ddot{q}_{\mathrm{f}} + C_{\mathrm{f}}\dot{q}_{\mathrm{f}} + N_{\mathrm{f}}(q_{\mathrm{f}}) = u_{\mathrm{f}}, \tag{5}$$

where (3) has been used. Note that N_{f} is a nonlinear term defined as $N_{\mathrm{f}} \triangleq N_{\mathrm{f}_{\mathrm{L}_2}}(q_{\mathrm{f}_{\mathrm{L}_2}}, \mathrm{s_f}) - N_{\mathrm{H}}(q_{\mathrm{H}}, \mathrm{H})$, where N_{H} is defined as $N_{\mathrm{H}} \triangleq \frac{m_{\mathrm{f}}}{m} N(q_{\mathrm{H}}, \mathrm{H})$.

Remark II.2 *The Coriolis matrix $C_{\rm f}$ satisfies the skew symmetric property of $x^TC_{\rm f}x=0$, $\forall x\in\mathbb{R}^3$.*

Remark II.3 *The left-hand side of (5) produces an affine parameterization $m_{\rm f}\ddot{q}_{\rm f}+C_{\rm f}\dot{q}_{\rm f}+N_{\rm f}(q_{\rm f})=Y(\ddot{q}_{\rm f},\dot{q}_{\rm f},q_{\rm f})m_{\rm f}$, where $m_{\rm f}$ is the unknown, constant mass of the follower spacecraft and $Y(\cdot)\in\mathbb{R}^3$ is a regression matrix defined as*

$$Y\triangleq\begin{bmatrix}\ddot{x}_{\rm f}-2\omega\dot{y}_{\rm f}-\omega^2x_{\rm f}+\frac{\mu_{\rm S}(x_{\rm f}+x_{\rm H}+R_{\rm L_2}+R_{\rm S})}{\|R_{\rm S\to s_f}\|^3}+\frac{\mu_{\rm E}(x_{\rm f}+x_{\rm H}+R_{\rm L_2}-R_{\rm E})}{\|R_{\rm E\to s_f}\|^3}-\frac{\mu_{\rm S}(x_{\rm H}+R_{\rm L_2}+R_{\rm S})}{\|R_{\rm S\to H}\|^3}-\frac{\mu_{\rm E}(x_{\rm H}+R_{\rm L_2}-R_{\rm E})}{\|R_{\rm E\to H}\|^3}\\ \ddot{y}_{\rm f}+2\omega\dot{x}_{\rm f}-\omega^2y_{\rm f}+\frac{\mu_{\rm S}(y_{\rm f}+y_{\rm H})}{\|R_{\rm S\to s_f}\|^3}+\frac{\mu_{\rm E}(y_{\rm f}+y_{\rm H})}{\|R_{\rm E\to s_f}\|^3}-\frac{\mu_{\rm S}\ y_{\rm H}}{\|R_{\rm S\to H}\|^3}-\frac{\mu_{\rm E}\ y_{\rm H}}{\|R_{\rm E\to H}\|^3}\\ \ddot{z}_{\rm f}+\frac{\mu_{\rm S}(z_{\rm f}+z_{\rm H})}{\|R_{\rm S\to s_f}\|^3}+\frac{\mu_{\rm E}(z_{\rm f}+z_{\rm H})}{\|R_{\rm E\to s_f}\|^3}-\frac{\mu_{\rm S}\ z_{\rm H}}{\|R_{\rm S\to H}\|^3}-\frac{\mu_{\rm E}\ z_{\rm H}}{\|R_{\rm E\to H}\|^3}\end{bmatrix}. \quad (6)$$

III. Spacecraft Formation Design

In this section, we exploit Ref. 10 to develop a method of designing reference trajectories for the follower spacecraft relative to the leader spacecraft on the Halo orbit trajectory. Specifically, we present a method of designing quasi-periodic orbits around a nominal Halo orbit. These quasi-periodic orbits will be used as the desired trajectories for the follower spacecraft. Furthermore, we will exploit special characteristics of these quasi-periodic orbits to parameterize spacecraft formations about the leader spacecraft on the Halo orbit.

We begin by expressing the relative position dynamics of (5) in a state-space form, i.e., let $x_1(t)\in\mathbb{R}^3$ be defined as $x_1\triangleq q_{\rm f}$ and $x_2(t)\in\mathbb{R}^3$ be defined as $x_2\triangleq\dot{q}_{\rm f}$. Then (5) can be written as

$$\dot{X}_{\rm f}=\begin{bmatrix}\dot{x}_1\\ \dot{x}_2\end{bmatrix}=\begin{bmatrix}x_2\\ -m_{\rm f}^{-1}\left(C_{\rm f}x_2+N_{\rm f}(x_1)\right)\end{bmatrix}, \quad (7)$$

where $X_{\rm f}(t)\triangleq\begin{bmatrix}x_1^T & x_2^T\end{bmatrix}^T\in\mathbb{R}^6$ and we assume that $u_{\rm f}=0$, $\forall t\geq 0$. Next, we linearize the nonlinear terms on the right hand side of (7), in the neighborhood of $X_{\rm f}=0$, to obtain

$$\dot{X}_{\rm f}=AX_{\rm f}, \quad (8)$$

where $A(t)\in\mathbb{R}^{6\times 6}$ is a time varying matrix with elements that are periodic with time. It is defined as $A\triangleq\begin{bmatrix}0_3 & \mathrm{I}_3\\ -m_{\rm f}^{-1}\frac{dN_{\rm f}(x_1)}{dx_1}\Big|_{x_1=0} & -m_{\rm f}^{-1}C_{\rm f}\end{bmatrix}$, where 0_3 is the 3×3 zero matrix, I_3 is the 3×3 identity matrix, and $\frac{dN_{\rm f}(x_1)}{dx_1}\Big|_{x_1=0}$ is the 3×3 Jacobian matrix of $N_{\rm f}(x_1)$ evaluated at $x_1=0$. In addition, the period of oscillation of A is the same as the period of the nominal Halo orbit, i.e., A is periodic with a frequency $\omega_{\rm H}$. Note that the time dependence of A characterizes the dynamics resulting from the linearization of (7) as a nonautonomous, linear differential equation with a periodic A matrix. Consequently, we employ Floquet theory[12] to transform (8) into an autonomous, linear differential equation so as to facilitate an explicit solution of (8).

We begin by introducing the notion of a fundamental matrix[12] of (8) denoted as $\varphi(t)\in\mathbb{R}^{6\times 6}$. Next, we denote the Halo orbit period as $T_{\rm H}$. Using Floquet theory, we utilize the transformation

$$X_{\rm f}=PY_{\rm f},\qquad Y_{\rm f}=P^{-1}X_{\rm f}, \quad (9)$$

where $Y_{\rm f}(t)\in\mathbb{R}^6$ is a vector composed of the transformed state $X_{\rm f}$ and $P(t)\in\mathbb{R}^{6\times 6}$ is a matrix with elements that are periodic with time,[12] to transform the nonautonomous differential equation of (8) into

$$\dot{Y}_{\rm f}=BY_{\rm f}, \quad (10)$$

where $B\in\mathbb{R}^{6\times 6}$ is a constant matrix. Following Ref. 12, the B matrix can be computed using φ and $T_{\rm H}$ as follows $B=\frac{1}{T_{\rm H}}\log\left(\varphi^{-1}(0)\varphi(T_{\rm H})\right)$, where the log function denotes the logarithm of a matrix. Furthermore,

the P matrix can be computed using φ and B as follows $P(t) = \varphi(t)e^{-Bt}$. Note that the P matrix is nonsingular $\forall t \in \mathbb{R}$, such that the transformation of (9) is unique.[13]

The autonomous, linear differential equation of (10) is equivalent to (8) in the transformed set of coordinates. Furthermore, the eigenvalues of the B matrix are denoted as the characteristic exponents,[13] which describe the stability characteristics of any trajectory that is sufficiently near the nominal Halo orbit. It is observed in Ref. 9 that direct computation of the eigenvalues of B results in a pair of hyperbolic eigenvalues, a pair of zero eigenvalues, and a pair of nonzero, pure, imaginary eigenvalues. We denote the pair of hyperbolic eigenvalues as λ_{h_1} and λ_{h_2} and the frequency corresponding to the nonzero, pure, imaginary eigenvalues as ω_{Q}. Next, we perform a coordinate transformation of the form

$$Y_{\mathrm{f}} = TZ_{\mathrm{f}}, \tag{11}$$

where $Z_{\mathrm{f}}(t) \in \mathbb{R}^6$ is a vector composed of the transformed state Y_{f} and $T \in \mathbb{R}^{6\times 6}$ is a time independent, linear transformation matrix, which transforms the B matrix into a modal matrix form, denoted by $\Omega \in \mathbb{R}^{6\times 6}$ defined as $\Omega \triangleq \mathrm{diag}\left\{ \begin{bmatrix} 0 & 1 \\ 0 & 0 \end{bmatrix}, \begin{bmatrix} 0 & 1 \\ -\lambda_{\mathrm{h}_1}\lambda_{\mathrm{h}_2} & (\lambda_{\mathrm{h}_1}+\lambda_{\mathrm{h}_2}) \end{bmatrix}, \begin{bmatrix} 0 & 1 \\ -\omega_{\mathrm{Q}}^2 & 0 \end{bmatrix} \right\}$. Then (10) is transformed into $\dot{Z}_{\mathrm{f}} = \Omega Z_{\mathrm{f}}$.

Now, it is trivial to obtain the following solution of Z_{f} analytically

$$Z_{\mathrm{f}} = \Bigg[Z_{\mathrm{f}_1}(0) + Z_{\mathrm{f}_2}(0)t \quad Z_{\mathrm{f}_2}(0) \quad \frac{-\lambda_{\mathrm{h}_2}Z_{\mathrm{f}_3}(0) + Z_{\mathrm{f}_4}(0)}{\lambda_{\mathrm{h}_1}-\lambda_{\mathrm{h}_2}}e^{\lambda_{\mathrm{h}_1}t} + \frac{\lambda_{\mathrm{h}_1}Z_{\mathrm{f}_3}(0) - Z_{\mathrm{f}_4}(0)}{\lambda_{\mathrm{h}_1}-\lambda_{\mathrm{h}_2}}e^{\lambda_{\mathrm{h}_2}t}$$
$$\frac{-\lambda_{\mathrm{h}_2}Z_{\mathrm{f}_3}(0) + Z_{\mathrm{f}_4}(0)}{\lambda_{\mathrm{h}_1}-\lambda_{\mathrm{h}_2}}\lambda_{\mathrm{h}_1}e^{\lambda_{\mathrm{h}_1}t} + \frac{\lambda_{\mathrm{h}_1}Z_{\mathrm{f}_3}(0) - Z_{\mathrm{f}_4}(0)}{\lambda_{\mathrm{h}_1}-\lambda_{\mathrm{h}_2}}\lambda_{\mathrm{h}_2}e^{\lambda_{\mathrm{h}_2}t} \quad D\cos(\omega_{\mathrm{Q}}t+\phi) \quad -D\omega_{\mathrm{Q}}\sin(\omega_{\mathrm{Q}}t+\phi) \Bigg]^T, \tag{12}$$

where $Z_{\mathrm{f}_i}(0)$, $i = 1, \ldots, 6$, denotes the i^{th} initial condition of the vector Z_{f} and $D, \phi \in \mathbb{R}$ are parameters that characterize size, location, and shape of the relative trajectory around the nominal Halo orbit. Eq. (12) reveals that the general solution of Z_{f} may not be periodic for arbitrary initial conditions. However, by properly choosing the initial condition $Z_{\mathrm{f}}(0)$ the terms corresponding to the pair of zero eigenvalues and the hyperbolic eigenvalues that produce unstable and/or asymptotically stable motion can be eliminated, thus resulting in periodic motion for Z_{f}. The remaining periodic terms in (12) allow the trajectory designer freedom to choose the parameters $Z_{\mathrm{f}_1}(0)$, D, and ϕ to satisfy mission specifications.

To compute the follower spacecraft trajectory relative to the nominal Halo orbit requires transformation from $Z_{\mathrm{f}} \longrightarrow X_{\mathrm{f}}$ in the form of

$$X_{\mathrm{f}} = PTZ_{\mathrm{f}}, \tag{13}$$

where (9) and (11) have been used. Note that the P matrix is composed of elements which are periodic with respect to time, with frequency ω_{H}, whereas the solution to Z_{f} is composed of elements which are periodic with respect to time, with frequency ω_{Q}. Consequently, the solution of X_{f} is a trajectory with two frequency components ω_{H} and ω_{Q}. It is observed that these frequencies ω_{Q} and ω_{H} are linearly independent, i.e., the condition $a_1\omega_{\mathrm{Q}} + a_2\omega_{\mathrm{H}} = 0$, $a_i \in \mathbb{Z}$, $i = 1, 2$, where $\mathbb{Z}$ is the set of integers, holds only for $a_i = 0$, $i = 1, 2$ (see Ref. 14 for details on linearly independent frequencies). Such a trajectory containing linearly independent frequency components are termed as quasi-periodic trajectories (see Ref. 14 for details on quasi-periodic functions). Thus, the X_{f} trajectory has the characteristic of being quasi-periodic. Finally, we utilize X_{f} as the desired trajectory of the follower spacecraft relative to the Halo orbit $q_{\mathrm{d_f}}(t) \in \mathbb{R}^3$, i.e., $\begin{bmatrix} q_{\mathrm{d_f}}^T & \dot{q}_{\mathrm{d_f}}^T \end{bmatrix}^T = X_{\mathrm{f}}$.

Remark III.1 *To facilitate subsequent illustrative examples, we approximate the Halo orbit and the P matrix using Fourier series approximations. Since both q_{H} and P are periodic with the same period, the resulting Fourier series approximations are convergent to the actual forms of q_{H} and P. To compute the time derivatives of q_{H} and P, we analytically differentiate the Fourier series approximations with respect to time. Thus, it follows that $q_{\mathrm{d_f}}$ and its time derivatives, viz., $\dot{q}_{\mathrm{d_f}}$ and $\ddot{q}_{\mathrm{d_f}}$ or equivalently $\dot{X}_{\mathrm{f}}$, are computed*

using q_{H}, P, and Z_{f}, and their time derivatives, i.e.,

$$\dot{X}_{\mathrm{f}} = \dot{P}TZ_{\mathrm{f}} + PT\dot{Z}_{\mathrm{f}}, \tag{14}$$

where (13) has been used.

IV. Trajectory Tracking Problem Formulation

In this section, we formulate a control design problem such that the follower spacecraft relative position q_{f} tracks a desired relative position trajectory $q_{\mathrm{d_f}}$, i.e., $\lim_{t\to\infty} q_{\mathrm{f}}(t) - q_{\mathrm{d_f}}(t) = 0$. The effectiveness of this control objective is quantified through the definition of a position tracking error $e(t) \in \mathbb{R}^3$ as

$$e \triangleq q_{\mathrm{f}} - q_{\mathrm{d_f}}. \tag{15}$$

The goal is to construct a control algorithm that obtains the aforementioned tracking result in the presence of the unknown constant follower spacecraft mass m_{f}. We assume that the position and velocity measurements (i.e., q_{f} and $\dot{q}_{\mathrm{f}}$) of the follower spacecraft relative to the leader spacecraft on a nominal Halo orbit are available for feedback.

To facilitate the control development, we assume that the desired trajectory $q_{\mathrm{d_f}}$ and its first two time derivatives are bounded functions of time. Next, we define the follower spacecraft mass estimation error $\tilde{m}_{\mathrm{f}}(t) \in \mathbb{R}$ as

$$\tilde{m}_{\mathrm{f}} \triangleq \hat{m}_{\mathrm{f}} - m_{\mathrm{f}}, \tag{16}$$

where $\hat{m}_{\mathrm{f}}(t) \in \mathbb{R}$ is the follower spacecraft mass estimate.

V. Adaptive Position Tracking Controller

In this section, we design an adaptive feedback control law that asymptotically tracks a pre-specified follower spacecraft relative position trajectory, in the presence of the unknown constant follower spacecraft mass m_{f}. In order to state the main result of this section, we define the following notation. A filter tracking error variable $r(t) \in \mathbb{R}^3$ is defined as

$$r \triangleq \dot{e} + \alpha e, \tag{17}$$

where $\alpha \in \mathbb{R}^{3\times 3}$ is a constant, diagonal, positive-definite, control gain matrix. In addition, an augmented error variable is defined as $\eta(t) \triangleq \begin{bmatrix} r^T & e^T \end{bmatrix}^T \in \mathbb{R}^6$ and a positive constant λ is defined as $\lambda \triangleq \min\{\lambda_{\min}\{K\}, \lambda_{\min}\{K_p\alpha\}\}$, where $\lambda_{\min}\{\cdot\}$ denotes the minimum eigenvalue of a matrix and $K, K_p \in \mathbb{R}^{3\times 3}$ are constant, diagonal, positive-definite matrices. Next, we solve for $\dot{e}$ in (17) to produce

$$\dot{e} = r - \alpha e. \tag{18}$$

Finally, we define a new regression matrix $Y_{\mathrm{d}}(\cdot) \in \mathbb{R}^3$ as $Y_{\mathrm{d}}(\cdot) \triangleq Y(\xi_1, \xi_2, q_{\mathrm{f}})$, where the linear parameterization of Remark II.3 has been used with $\xi_1 = \ddot{q}_{\mathrm{d_f}} - \alpha\dot{e}$ and $\xi_2 = \dot{q}_{\mathrm{d_f}} - \alpha e$, in the definition of (6).

Theorem V.1 *Let $K, K_p \in \mathbb{R}^{3\times 3}$ be constant, diagonal, positive-definite matrices and $\Gamma \in \mathbb{R}$ be a positive constant. Then, the adaptive control law*

$$u_{\mathrm{f}} = Y_{\mathrm{d}}\hat{m}_{\mathrm{f}} - K_p e - Kr, \quad \dot{\hat{m}}_{\mathrm{f}} = -\Gamma Y_{\mathrm{d}}^T r, \tag{19}$$

ensures global asymptotic convergence of the position and velocity tracking errors as delineated by $\lim_{t\to\infty} e(t)$, $\dot{e}(t) = 0$.

Proof. We begin by rewriting the follower spacecraft relative position dynamics (5) in terms of the filtered tracking error variable (17). To this end, differentiating (17) with respect to time, multiplying both sides of the resulting equation by $m_{\rm f}$, using $\ddot{e} = \ddot{q}_{\rm f} - \ddot{q}_{\rm d_f}$ from (15), substituting for $m_{\rm f}\ddot{q}_{\rm f}$ from (5), and rearranging terms yield

$$m_{\rm f}\dot{r} = -m_{\rm f}(\ddot{q}_{\rm d_f} - \alpha\dot{e}) - C_{\rm f}\dot{q}_{\rm f} - N_{\rm f}(q_{\rm f}) + u_{\rm f}. \tag{20}$$

Next, we expand (17) by noting that $\dot{e} = \dot{q}_{\rm f} - \dot{q}_{\rm d_f}$. Then solving for $\dot{q}_{\rm f}$, substituting the result into (20), and rearranging terms, we get

$$m_{\rm f}\dot{r} = -m_{\rm f}(\ddot{q}_{\rm d_f} - \alpha\dot{e}) - C_{\rm f}(\dot{q}_{\rm d_f} - \alpha e) - N_{\rm f}(q_{\rm f}) - C_{\rm f}r + u_{\rm f} = -Y_{\rm d}m_{\rm f} - C_{\rm f}r + u_{\rm f}, \tag{21}$$

where the definition of $Y_{\rm d}$ has been used. Eq. (21) characterizes the open-loop dynamics of r. Now, substituting $u_{\rm f}$ of (19) into (21) results in the following closed-loop dynamics for r

$$m_{\rm f}\dot{r} = Y_{\rm d}\tilde{m}_{\rm f} - K_p e - Kr - C_{\rm f}r, \tag{22}$$

where the definition of (16) has been used. Finally, note that differentiating (16) with respect to time and using $\dot{\hat{m}}_{\rm f}$ of (19), produce the closed-loop dynamics for the spacecraft mass estimation error

$$\dot{\tilde{m}}_{\rm f} = -\Gamma Y_{\rm d}^T r. \tag{23}$$

Now, we utilize the error systems of (22) and (23) along with the positive-definite, candidate Lyapunov function defined by $V \triangleq \frac{1}{2}m_{\rm f}r^Tr + \frac{1}{2}e^TK_pe + \frac{1}{2\Gamma}\tilde{m}_{\rm f}^2$, to prove the above stability result for the position and velocity tracking errors. Specifically, differentiating V with respect to time and substituting the closed-loop dynamics of (18) and (22) into the result, we obtain

$$\dot{V} = -r^TKr - e^TK_p\alpha e \leq -\lambda\|\eta\|^2 \leq 0, \tag{24}$$

where the property of Remark II.2, (23), and the definitions of η and λ have been used.

Since V is a non-negative function and $\dot{V}$ is a negative semi-definite function, V is a non-increasing function. Thus $V(t) \in \mathcal{L}_\infty$ as described by $V(r(t), e(t), \tilde{m}_{\rm f}(t)) \leq V(r(0), e(0), \tilde{m}_{\rm f}(0))$, $t \geq 0$. Using standard signal chasing arguments, all signals in the closed-loop system can now be shown to be bounded. Using (18) and (22) along with the boundedness of all signals in the closed-loop system, we now conclude that $\dot{\eta} \in \mathcal{L}_\infty$. Solving the differential inequality of (24) results in $V(0) - V(\infty) \geq \lambda\int_0^\infty \|\eta(t)\|^2dt$.

Since $V(t)$ is bounded, $t \geq 0$, we conclude that $\eta(t) \in \mathcal{L}_\infty \bigcap \mathcal{L}_2$, $t \geq 0$. Finally, using Barbalat's Lemma,[15] we conclude that $\lim_{t\to\infty}\eta(t) = 0$. Using the definitions of r and η, $\lim_{t\to\infty}\eta(t) = 0$, and Lemma 1.6 of Ref. 15, yield the result of Theorem V.1. □

VI. Simulation Results

In this section, we present illustrative examples that incorporate the algorithms presented in Sections III and V. Specifically, we provide details on computing the quasi-periodic trajectories described in Section III. Next, we provide a simulation of the follower spacecraft relative dynamics (5), utilizing the control and adaptation laws of (19) so that the follower spacecraft tracks a desired quasi-periodic trajectory relative to a nominal Halo orbit.

In all simulations, we employ the Sun-Earth system circular orbit parameters:[7,16] $G = 6.671\times10^{-11}\frac{\rm m^3}{\rm kg\cdot s^2}$, $\omega = 2.73774795629 \times 10^{-3}\frac{\rm rad}{\rm day}$, $M_{\rm S} = 1.9891 \times 10^{30}$kg, $M_{\rm E} = 5.974 \times 10^{24}$kg, 1 AU $= 1.496 \times 10^{8}$km, and $R_{\rm L_2} = 1.010033599267463$ AU, where 1 AU stands for 1 Astronomical Unit denoting the distance between the Sun and the Earth. Furthermore, we consider that the follower spacecraft has a mass of $m_{\rm f} = 1000$kg. Finally, the distances $R_{\rm S}$ and $R_{\rm E}$ can be computed as $R_{\rm S} = \frac{M_{\rm E}}{M_{\rm E}+M_{\rm S}} \times 1$AU and $R_{\rm E} = \frac{M_{\rm S}}{M_{\rm E}+M_{\rm S}} \times 1$AU.

A. Quasi-Periodic Trajectory Generation

Applying the numerical algorithm presented in Subsection B results in a family of initial conditions for the Halo orbit from which we have selected the following initial condition $q_{\mathrm{H}}(0) = [-2.61921376240742\ 0\ -0.13648677396294] \times 10^5$km and $\dot{q}_{\mathrm{H}}(0) = [0\ 4.21353617291110\ 0] \times 10^3 \frac{\mathrm{km}}{\mathrm{day}}$. In addition, the Halo orbit period is determined to be $T_{\mathrm{H}} = 1.135225027876099 \times 10^3$day. Figure 1(b) shows the Halo orbit relative to the L_2 Lagrange point and its projections onto the $\{x_{\mathrm{L}_2}, y_{\mathrm{L}_2}\}$, $\{x_{\mathrm{L}_2}, z_{\mathrm{L}_2}\}$, and $\{y_{\mathrm{L}_2}, z_{\mathrm{L}_2}\}$ planes. In addition, we utilized 25 terms of a Fourier series to approximate the Halo orbit trajectory q_{H}. The fundamental matrix φ described in Section III is numerically computed using $A(t)$ as follows $\dot{\varphi} = A(t)\varphi$, $\varphi(0) = \mathrm{I}_6$, $\forall t \in [0, T_{\mathrm{H}}]$. Thus, using $P(t) = \varphi(t)e^{-Bt}$, P is numerically computed $\forall t \in [0, T_{\mathrm{H}}]$. Next, we compute a Fourier series approximation of P, where we retain 25 terms of the series approximation. This, along with the analytic expression for Z_{f} is used to compute $q_{\mathrm{d_f}}$ and its time derivatives analytically from (14).

To show the resulting trajectories of $q_{\mathrm{d_f}}$, given different numerical values for parameters $Z_{\mathrm{f_1}}(0)$, D, and ϕ, we simulated $q_{\mathrm{d_f}}$ using a parameter set: $Z_{\mathrm{f_1}}(0) = 0$, $D = 0.0001$, and $\phi = 0$ rad. By computing the eigenvalues of the B matrix, we determined $\omega_{\mathrm{Q}} = 6.286301816644046 \times 10^{-5} \frac{1}{\mathrm{day}}$. Figure 2(a) shows the quasi-periodic trajectory relative to the nominal Halo orbit for parameter values of $\phi = 0$, $\phi = \frac{\pi}{4}$, and $\phi = \frac{\pi}{2}$. Figure 2(a) illustrates that changes in ϕ denote changes in the initial position of the spacecraft along a given quasi-periodic trajectory. Next, we simulated $q_{\mathrm{d_f}}$ using a parameter set: $Z_{\mathrm{f_1}}(0) = 0$, $D = 0.0002$, and $\phi = 0$ rad. Figure 2(b) shows the desired quasi-periodic trajectory relative to the nominal Halo orbit. Note that the parameter D determines the size and shape of the desired quasi-periodic trajectory relative to the nominal Halo orbit. We also simulated $q_{\mathrm{d_f}}$ using a parameter set: $Z_{\mathrm{f_1}}(0) = 0.0001$, $D = 0$, and $\phi = 0$ rad. For this parameter set, Figure 2(c) shows a periodic trajectory relative to the nominal Halo orbit with the same period as ω_{H}. Finally, we simulated $q_{\mathrm{d_f}}$ using a parameter set: $Z_{\mathrm{f_1}}(0) = 0.0001$, $D = 0.0001$, and $\phi = 0$ rad. For this parameter set, Figure 2(d) shows the quasi-periodic trajectory relative to the nominal Halo orbit.

B. Adaptive Full-State Feedback Control of Follower Spacecraft

The adaptive control law of (19) was simulated for the follower spacecraft dynamics relative to the leader spacecraft on a nominal Halo orbit (5). When tracking desired quasi-periodic trajectories, we initialized the follower spacecraft with the set of initial conditions given as $q_{\mathrm{f}}(0) = [-2.61921376240742\ -2.57780484325713\ -0.13648677396294] \times 10^5$km and $\dot{q}_{\mathrm{f}}(0) = [-0.01469110370264\ 4.21353617291110\ -0.01469092330256] \times 10^3 \frac{\mathrm{km}}{\mathrm{day}}$. The control and adaptation gains are obtained through trial and error in order to obtain good performance for the tracking error response. The following resulting gains were used in this simulation $K = \mathrm{diag}\,(1,1,1) \times 1.499 \times 10$, $K_p = \mathrm{diag}\,(1,1,1) \times 5.475 \times 10^3$, $\alpha = \mathrm{diag}\,(1,1,1) \times 8.213 \times 10^{-2}$, and $\Gamma = 8.888 \times 10^4$. In addition, the follower spacecraft mass parameter estimate was initialized to $\hat{m}_{\mathrm{f}}(0) = 600$ kg. A simulation of the follower spacecraft tracking the desired quasi-periodic trajectory of Figure 2(a) is performed. The trajectory q_{f} is shown in Figures 2(e) and 2(f). Figure 3 shows the position tracking error e and the velocity tracking error $\dot{e}$. The control input u_{f} is shown in Figure 4(a). Finally, the follower spacecraft mass estimate $\hat{m}_{\mathrm{f}}$ is shown in Figure 4(b).

VII. Conclusion

In this paper, we designed desired quasi-periodic trajectories for the follower spacecraft relative to the leader spacecraft on the Halo orbit. The size, location, and shape of these trajectories were characterized by a set of parameters. Illustrative simulations were performed to show these parameter characteristics. Next, a Lyapunov design was used to develop an adaptive full-state feedback controller, which yielded global, asymptotic convergence of the relative position tracking errors. Simulation results were presented to show good trajectory tracking.

Acknowledgements

Research supported in part by the National Aeronautics and Space Administration–Goddard Space Flight Center under Grant NGT5-151 and the New York Space Grant Consortium under Grant 39555-6519.

References

[1]H. K. Hills, "International Sun-Earth Explorers Project Information," *National Space Science Data Center* [online database], URL: http://nssdc.gsfc.nasa.gov/space/isee.html.

[2]K. C. Howell, B. T. Barden, R. S. Wilson, and M. W. Lo, "Trajectory Design using a Dynamical Systems approach with Application to Genesis," *Proceedings of the AAS/AIAA Astrodynamics Specialist Conference,* Sun Valley, ID, 1997, AAS Paper 97–709.

[3]P. A. Sabelhaus and J. Decker, "An Overview of the James Webb Space Telescope (JWST) Project," *Proceedings of SPIE*, Vol. 5487, Paper No. 21, June 2004.

[4]C. V. M. Fridlund, "Darwin–The Infrared Space Interferometry Mission," *ESA Bulletin*, Vol. 103, pp. 20–25, 2000.

[5]D. L. Richardson, "Analytic Construction of Periodic Orbits about the Collinear Points," *Celestial Mechanics*, Vol. 22, pp. 241-253, 1980.

[6]V. Szebehely, *Theory of Orbits.* New York, NY: Academic Press, 1967.

[7]R. Thurman and P. A. Worfolk, *The Geometry of Halo Orbits in the Circular Restricted Three-Body Problem*, Geometry Center Research Report GCG95, University of Minnesota, 1996.

[8]F. Y. Hsiao and D. J. Scheeres, "Design of Spacecraft Formation Orbits Relative to a Stabilized Trajectory," *AAS/AIAA Space Flight Mechanics Meeting,* AAS Paper 03-175, 2003.

[9]D. J. Scheeres, F. Y. Hsiao, and N. X. Vinh, "Stabilizing Motion Relative to an Unstable Orbit: Applications to Spacecraft Formation Flight," *Journal of Guidance, Control, and Dynamics*, Vol. 26, No. 1, pp. 62–73, 2003.

[10]G. Gomez, J. Masdemont, C. Simo, "Lissajous Orbits around Halo Orbits," *AAS/AIAA Space Flight Mechanics Meeting,* AAS Paper 97-106, 1997.

[11]H. Wong and V. Kapila, "Adaptive Nonlinear Control of Spacecraft Near Sun-Earth L_2 Lagrange Point," *Proceedings of the American Control Conference*, Denver, CO, pp. 1116–1121, 2003.

[12]C. T. Chen, *Linear System Theory and Design*, Oxford University Press, Oxford, NY, 1999.

[13]E. A. Coddington and N. Levinson, *Theory of Ordinary Differential Equations*, McGraw Hill, New York, NY, 1955.

[14]H. Bohr, *Almost Periodic Functions*, Springer, Berlin, 1933.

[15]D. M. Dawson, J. Hu, and T. C. Burg, *Nonlinear Control of Electric Machinery,* Marcel Dekker, New York, 1998.

[16]D. A. Vallado, *Fundamentals of Astrodynamics and Applications.* McGraw-Hill, 1997.

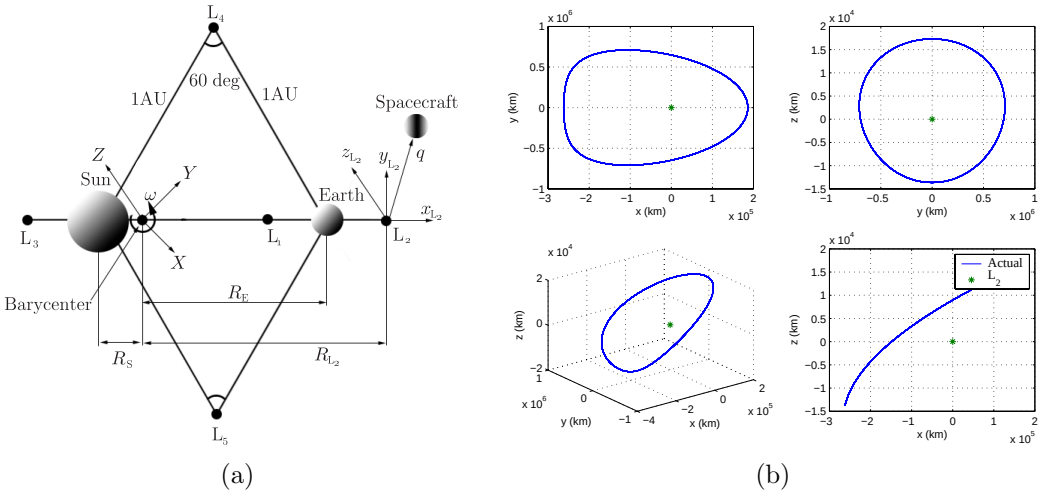

(a) (b)

Figure 1. (a) Sun-Earth system schematic diagram and (b) Halo orbit trajectory of the leader spacecraft relative to the L_2 Lagrange point

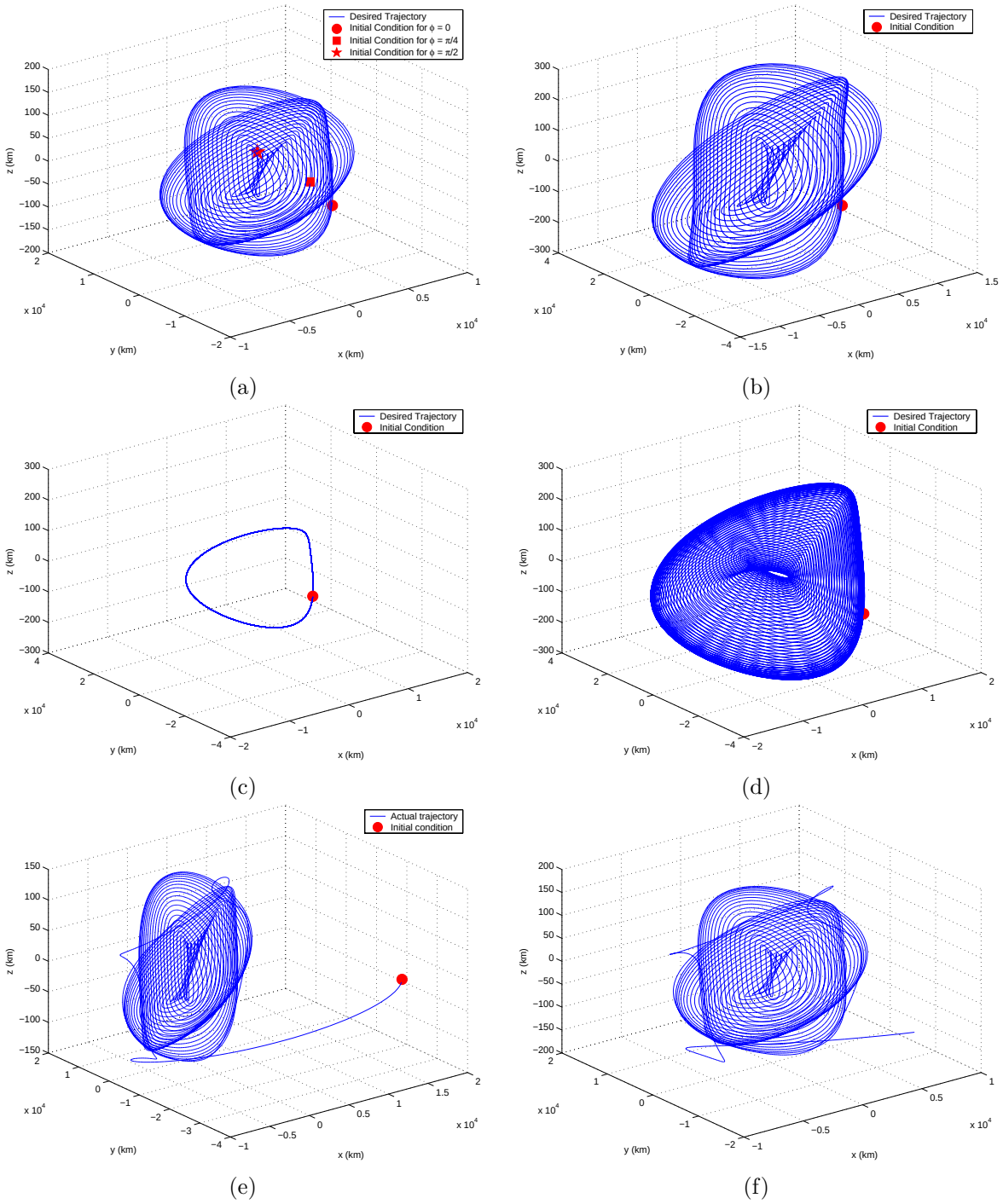

Figure 2. Trajectory of the follower spacecraft relative to the nominal Halo orbit using: (a) $Z_{f_1}(0) = 0, D = 0.0001, \phi = 0, \phi = \frac{\pi}{4}$, and $\phi = \frac{\pi}{2}$, (b) $Z_{f_1}(0) = 0, D = 0.0002, \phi = 0$, (c) $Z_{f_1}(0) = 0.0001$, $D = 0$, $\phi = 0$, (d) $Z_{f_1}(0) = 0.0001$, $D = 0.0001$, $\phi = 0$, (e) normal view, and (f) zoomed in view

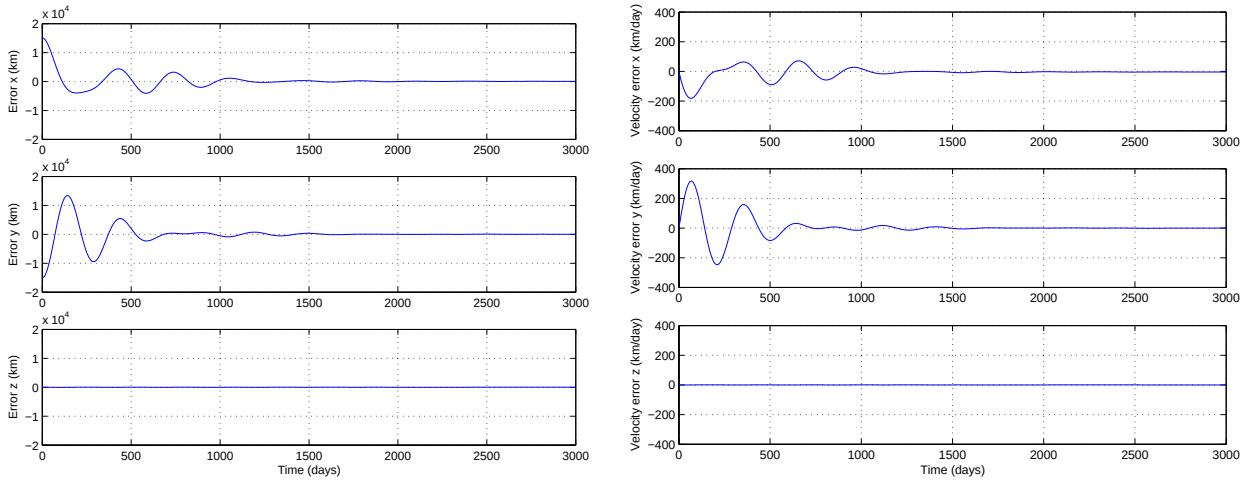

(a) (b)

Figure 3. (a) Position tracking error and (b) velocity tracking error

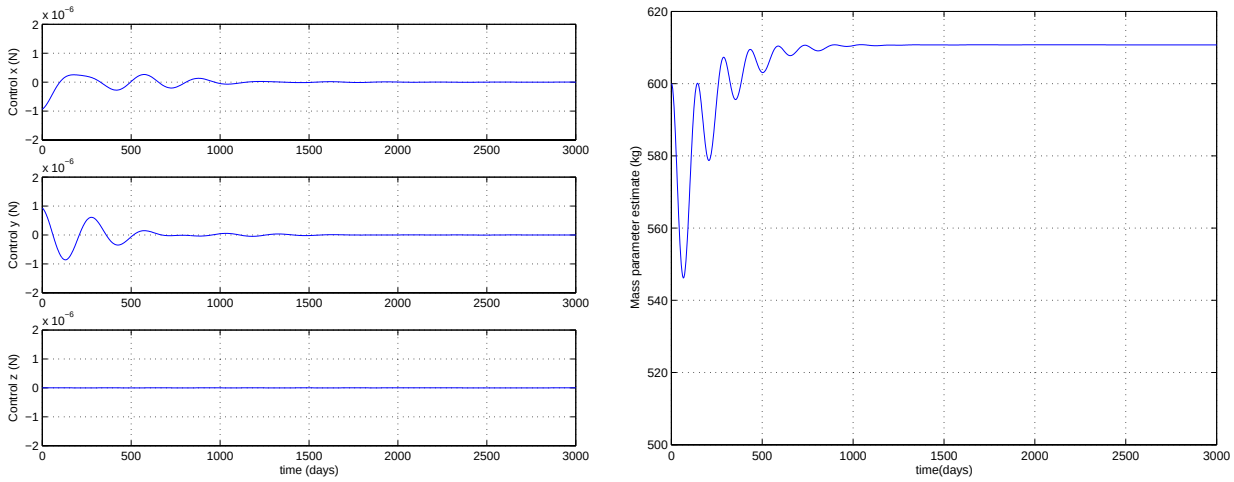

(a) (b)

Figure 4. Follower spacecraft (a) control input and (b) mass parameter estimate

HOME

Spacecraft Formation Flying near Sun-Earth L_2 Lagrange Point: Trajectory Generation and Adaptive Full-State Feedback Control

Hong Wong and Vikram Kapila

Polytechnic University

Brooklyn, NY 11201

2004 Formation Flying Symposium
Washington, DC
September 14-16, 2004

Poster Session

Motivation: Space Missions near Lagrange Points

- Lagrange points of the Sun-Earth system have been exploited as key locations for space-based astronomical observation stations
- Spacecraft operating in the vicinity of Lagrange point observation stations obtain nearly an unobstructed view of the galaxy
- Lagrange point missions are sufficiently far from the Earth such that environmental effects (e.g., atmospheric and geomagnetic forces) do not affect spacecraft dynamics
- Some future space missions to L_2 Lagrange point:
  - NGST: mission for deep-space observations and/or interstellar communication
    - Solar influences on the spacecraft are minimal
    - Space observations can be conducted on a frequent basis
  - Darwin: mission to search for life in the universe and investigate the evolution of galaxies
    - Incorporates six spacecraft to cooperatively work together in order to search nearby planets for traces of life in the form of infrared radiation

Motivation: Spacecraft Formation Flying

- Spacecraft formation flying (SFF): an emerging technology to enhance space-based imaging/interferometry missions
  - Enhances space mission performance by distributing mission tasks, usually conducted by a monolithic spacecraft, to many small spacecraft
  - Effective use of SFF for space missions near the Sun-Earth Lagrange points requires:
    * Proper design of spacecraft formations
    * Precise formation control

Goals

- Develop mathematical model for the follower spacecraft relative to the leader spacecraft
- Generate follower spacecraft trajectories relative to the leader spacecraft orbit to create a spacecraft formation
- Track desired reference trajectories in the presence of unknown follower spacecraft mass using:
  - Full-state feedback control law
  - Parameter update algorithm

Prior Research

- SFF trajectory designs near L_2 Lagrange point:
  - Reference trajectories for follower spacecraft were computed using classical orbital elements resulting in bounded orbits around the leader spacecraft on a periodic orbit: Hsiao and Scheeres, '03
  - Feedback control was utilized to produce reference trajectories for follower spacecraft: Scheeres *et. al.*, '03
  - Provided a method of generating reference trajectories for follower spacecraft using a numerical method, where the resulting trajectories are quasi-periodic: Gomez *et. al.*, '97
- Spacecraft control near Sun-Earth Lagrange points:
  - Floquet mode control tailors control inputs to cancel instability for spacecraft near Lagrange points: Simo *et. al.*, '86
  - Impulsive control inputs are generated using error feedback and by minimizing a cost function: Howell and Pernicka, '93
  - Control design utilizing nonlinear dynamics while accounting for elliptical Sun-Earth motion as perturbations: Giamberardino and Monaco, '92

Representation of Sun-Earth Lagrange points

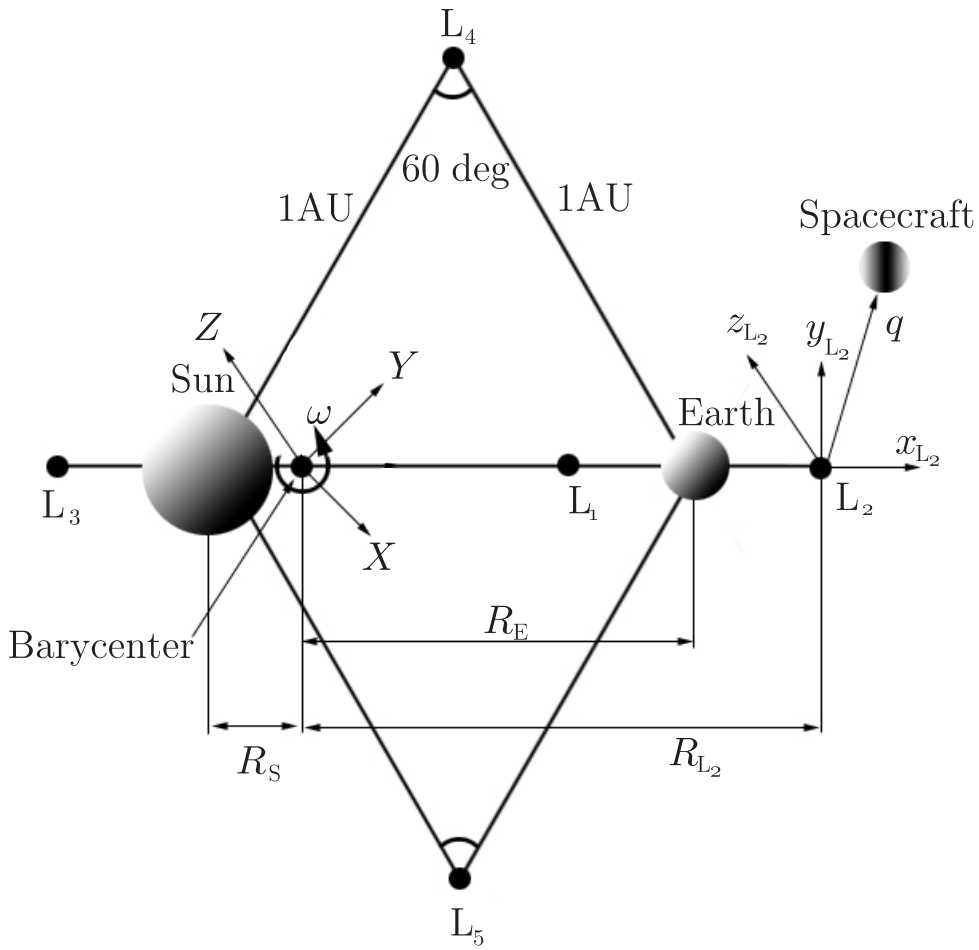

Dynamics Model of Spacecraft

- The mathematical model describing the position of a spacecraft relative to the L_2 Lagrange point is (Wong and Kapila, '03)

$$m\ddot{q} + C\dot{q} + N(q, \mathrm{s}) = u$$

  - m: spacecraft mass
  - C: coriolis-like matrix
  - N: gravitation term
  - u: control input

- The mathematical model describing the position of the follower spacecraft relative to the L_2 Lagrange point is

$$m_{\mathrm{f}}\ddot{q}_{\mathrm{f}_{L_2}} + C_{\mathrm{f}}\dot{q}_{\mathrm{f}_{L_2}} + N_{\mathrm{f}_{L_2}}(q_{\mathrm{f}_{L_2}}, \mathrm{s_f}) = u_{\mathrm{f}}$$

  - m_{f}: follower spacecraft mass
  - C_{f}: coriolis-like matrix
  - $N_{\mathrm{f}_{L_2}}$: gravitation term
  - u_{f}: follower spacecraft control input
  - $q_{\mathrm{f}_{L_2}}$: follower spacecraft position relative to the L_2 Lagrange point

- Assumption: leader spacecraft is on a Halo orbit

Halo Orbit Generation

- Generate Halo orbits using numerical methods (Richardson, '80)
  - Apply Poincare-Lindstedt method to obtain analytic approximations to a thrust-free periodic trajectory in a neighborhood of L_2 Lagrange point
  - Utilize analytic trajectories from Poincare-Lindstedt method to obtain an initial guess to an initial condition of a thrust-free periodic orbit
  - Utilize Newton's method to update initial conditions until it provides a set of initial conditions that leads to a trajectory that is nearly periodic
  - Propogate spacecraft dynamics relative to the L_2 Lagrange point using the initial conditions obtained from the algorithm
- The Halo orbit trajectory satisfies the spacecraft dynamics under the condition that the spacecraft control input is zero
- The leader spacecraft dynamics on the Halo orbit is given by

$$m\ddot{q}_{\mathrm{H}} + C\dot{q}_{\mathrm{H}} + N(q_{\mathrm{H}}, \mathrm{H}) = 0$$

Halo Orbit Generation

- Halo orbit relative to the L_2 Lagrange point

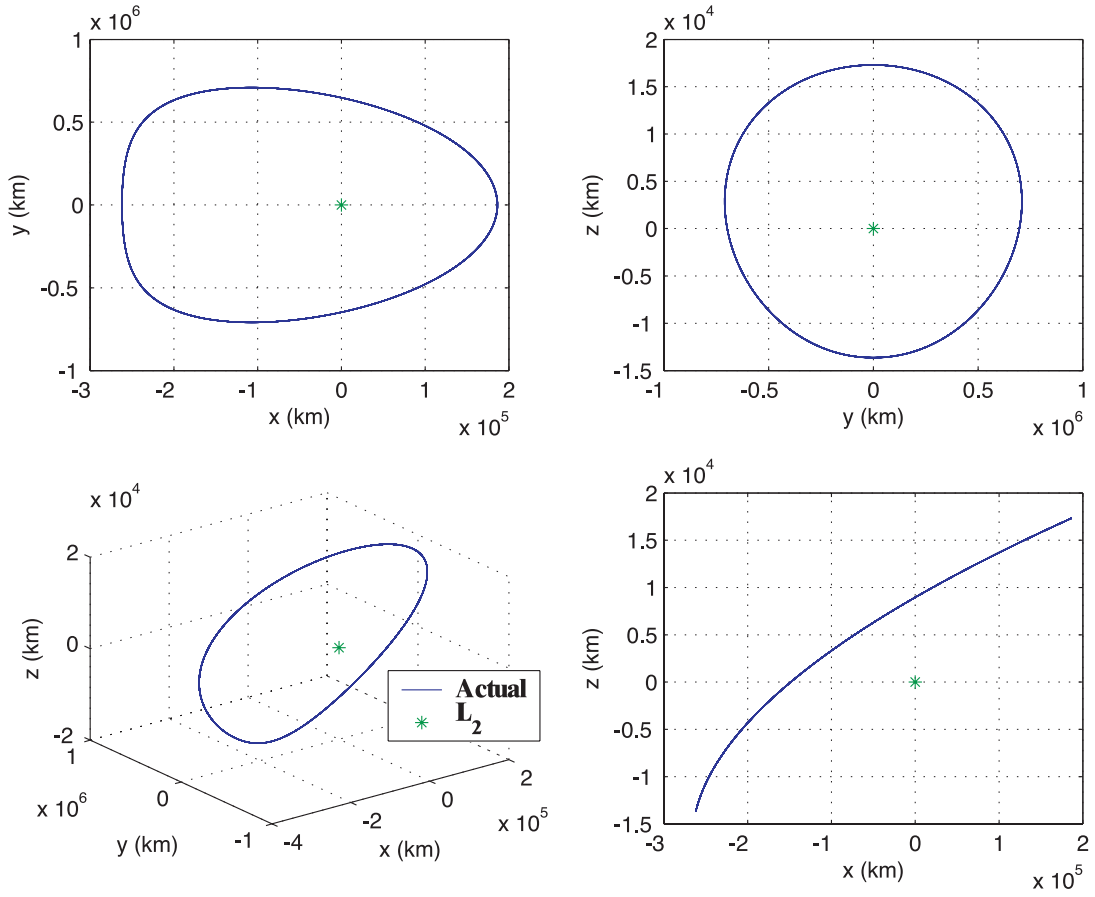

Follower Spacecraft Relative Dynamics Model

- Define the relative position between the follower and the leader spacecraft as $q_{\mathrm{f}} \stackrel{\triangle}{=} q_{\mathrm{f}_{\mathrm{L}_2}} - q_{\mathrm{H}}$

- Dynamics of the follower spacecraft position relative to the leader spacecraft

$$m_{\mathrm{f}}\ddot{q}_{\mathrm{f}} + C_{\mathrm{f}}\dot{q}_{\mathrm{f}} + N_{\mathrm{f}}(q_{\mathrm{f}}) = u_{\mathrm{f}}$$

  - $N_{\mathrm{f}} \stackrel{\triangle}{=} N_{\mathrm{f}_{\mathrm{L}_2}}(q_{\mathrm{f}_{\mathrm{L}_2}}, \mathrm{s}_{\mathrm{f}}) - N_{\mathrm{H}}(q_{\mathrm{H}}, \mathrm{H})$

- Key properties

  - Coriolis matrix satisfies skew-symmetry property

$$v^T C_{\mathrm{f}} v = 0, \qquad \forall\ v \in \mathbb{R}^3$$

  - Linear parameterization of nonlinear dynamics

$$m_{\mathrm{f}}\ddot{q}_{\mathrm{f}} + C_{\mathrm{f}}\dot{q}_{\mathrm{f}} + N_{\mathrm{f}}(q_{\mathrm{f}}) = Y(\ddot{q}_{\mathrm{f}}, \dot{q}_{\mathrm{f}}, q_{\mathrm{f}})m_{\mathrm{f}}$$

Spacecraft Formation Design: Linearization

- Express the relative position dynamics in a state-space form

$$\dot{X}_{\mathrm{f}} = \begin{bmatrix} \dot{x}_1 \\ \dot{x}_2 \end{bmatrix} = \begin{bmatrix} x_2 \\ -m_{\mathrm{f}}^{-1}\left(C_{\mathrm{f}} x_2 + N_{\mathrm{f}}(x_1)\right) \end{bmatrix}$$

$$u_{\mathrm{f}} = 0,\ \forall t \geq 0, \qquad x_1 \stackrel{\triangle}{=} q_{\mathrm{f}}, \qquad x_2 \stackrel{\triangle}{=} \dot{q}_{\mathrm{f}}$$

- Linearize nonlinear terms in the NBHD of $X_{\mathrm{f}} = 0$

$$\dot{X}_{\mathrm{f}} = AX_{\mathrm{f}}, \qquad A \stackrel{\triangle}{=} \begin{bmatrix} 0_3 & \mathrm{I}_3 \\ -m_{\mathrm{f}}^{-1}\frac{dN_{\mathrm{f}}(x_1)}{dx_1}\Big|_{x_1=0} & -m_{\mathrm{f}}^{-1}C_{\mathrm{f}} \end{bmatrix}$$

  - $\frac{dN_{\mathrm{f}}(x_1)}{dx_1}\Big|_{x_1=0}$: 3×3 Jacobian matrix of $N_{\mathrm{f}}(x_1)$ evaluated at $x_1 = 0$
  - $A(t)$: time varying matrix with periodic elements
    - Period of A same as the periodic nominal Halo orbit (denoted as T_{H})
  - $\varphi(t)$: fundamental matrix of the linearized, nonautonomous system

Spacecraft Formation Design: Floquet Theory

- Floquet transformation $X_\mathrm{f} = PY_\mathrm{f}$ from nonautonomous, linear ODE to autonomous, linear ODE

$$\dot{Y}_\mathrm{f} = BY_\mathrm{f}$$

  - $Y_\mathrm{f}(t)$: transformed state of X_f
  - B : constant matrix computed using φ and T_H as $B = \frac{1}{T_\mathrm{H}} \log\left(\varphi^{-1}(0)\varphi(T_\mathrm{H})\right)$
  - $P(t)$: matrix with periodic elements computed using φ and B as $P(t) = \varphi(t)e^{-Bt}$
  - Eigenvalues of B are denoted as characteristic exponents:
    - Pair of hyperbolic eigenvalues denoted as λ_{h_1} and λ_{h_2}
    - Pair of zero eigenvalues
    - Pair of nonzero, pure, imaginary eigenvalues (with frequency ω_Q)

Spacecraft Formation Design: Analytical Solution

- Perform a coordinate transformation of the form $Y_{\mathrm{f}} = TZ_{\mathrm{f}}$
  - $Z_{\mathrm{f}}(t)$: transformed state Y_{f} – T: time independent, transformation matrix
- B matrix is transformed into modal matrix form

$$\Omega \underline{=}^{\triangle} \mathrm{diag}\left\{ \begin{bmatrix} 0 & 1 \\ 0 & 0 \end{bmatrix}, \begin{bmatrix} 0 & 1 \\ -\lambda_{\mathrm{h}_1}\lambda_{\mathrm{h}_2} & (\lambda_{\mathrm{h}_1} + \lambda_{\mathrm{h}_2}) \end{bmatrix}, \begin{bmatrix} 0 & 1 \\ -\omega_{\mathrm{Q}}^2 & 0 \end{bmatrix} \right\}$$

- Analytical solution of Z_{f}

$$Z_{\mathrm{f}} = \begin{bmatrix} Z_{\mathrm{f}_1}(0) + Z_{\mathrm{f}_2}(0)t \\ Z_{\mathrm{f}_2}(0) \\ \frac{-\lambda_{\mathrm{h}_2} Z_{\mathrm{f}_3}(0) + Z_{\mathrm{f}_4}(0)}{\lambda_{\mathrm{h}_1} - \lambda_{\mathrm{h}_2}} e^{\lambda_{\mathrm{h}_1} t} + \frac{\lambda_{\mathrm{h}_1} Z_{\mathrm{f}_3}(0) - Z_{\mathrm{f}_4}(0)}{\lambda_{\mathrm{h}_1} - \lambda_{\mathrm{h}_2}} e^{\lambda_{\mathrm{h}_2} t} \\ \frac{-\lambda_{\mathrm{h}_2} Z_{\mathrm{f}_3}(0) + Z_{\mathrm{f}_4}(0)}{\lambda_{\mathrm{h}_1} - \lambda_{\mathrm{h}_2}} \lambda_{\mathrm{h}_1} e^{\lambda_{\mathrm{h}_1} t} + \frac{\lambda_{\mathrm{h}_1} Z_{\mathrm{f}_3}(0) - Z_{\mathrm{f}_4}(0)}{\lambda_{\mathrm{h}_1} - \lambda_{\mathrm{h}_2}} \lambda_{\mathrm{h}_2} e^{\lambda_{\mathrm{h}_2} t} \\ D\cos(\omega_{\mathrm{Q}} t + \phi) \\ -D\omega_{\mathrm{Q}} \sin(\omega_{\mathrm{Q}} t + \phi) \end{bmatrix}$$

  - $Z_{\mathrm{f}_i}(0)$, $i = 1, \ldots, 6$, denotes the i^{th} initial condition of Z_{f}
  - D, ϕ characterize size, location, and shape of the relative trajectory around the nominal Halo orbit

Spacecraft Formation Design: Quasi-Periodic Trajectories

- Solution of Z_{f} reveals that the general solution may not be periodic for arbitrary initial conditions
  - Proper choice of $Z_{\mathrm{f}}(0)$ will cancel non-periodic motion
- To compute the follower spacecraft trajectory relative to the nominal Halo orbit requires transformation from $Z_{\mathrm{f}} \longrightarrow X_{\mathrm{f}}$:

$$X_{\mathrm{f}} = PTZ_{\mathrm{f}}$$

- X_{f} is a trajectory with two frequency components ω_{H} and ω_{Q}
  - Linearly independent frequencies ω_{Q} and ω_{H}:
    - $a_1\omega_{\mathrm{Q}} + a_2\omega_{\mathrm{H}} = 0, \quad a_i \in \mathbb{Z}, \quad i = 1, 2, \quad$ holds only for $\quad a_i = 0, \quad i = 1, 2$
  - Quasi-periodic trajectories

Trajectory Tracking Problem Formulation

- Design control $u_{\mathrm{f}} \ni \lim_{t\to\infty} q_{\mathrm{f}}(t) - q_{\mathrm{d_f}}(t) = 0$
  - $q_{\mathrm{d_f}}$: desired quasi-periodic reference trajectory of the follower spacecraft relative to the Halo orbit
- Constraints
  - No knowledge of follower spacecraft mass
- Quantify control objective
  - Position tracking error: $e \triangleq q_{\mathrm{f}} - q_{\mathrm{d_f}}$
  - Follower spacecraft mass estimation error: $\tilde{m}_{\mathrm{f}} \triangleq \hat{m}_{\mathrm{f}} - m_{\mathrm{f}}$
    - $\hat{m}_{\mathrm{f}}(t)$: follower spacecraft mass estimate
- Filter tracking error: $r \triangleq \dot{e} + \alpha e$
- Augmented error variable: $\eta \triangleq \begin{bmatrix} r^T & e^T \end{bmatrix}^T$

Adaptive Position Tracking Control Design

- Control input:

$$u_{\mathrm{f}} = \underbrace{Y_{\mathrm{d}}\hat{m}_{\mathrm{f}}}_{\text{Feed-Forward Adaptation}} \quad \underbrace{-Kr}_{\text{Position-Velocity Error Feedback}} \quad \underbrace{-K_p e}_{\text{Position Error Feedback}}$$

  - New regression matrix: $Y_{\mathrm{d}}(\cdot) \triangleq Y(\ddot{q}_{\mathrm{d_f}} - \alpha\dot{e}, \dot{q}_{\mathrm{d_f}} - \alpha e, q_{\mathrm{f}})$

- Follower spacecraft mass estimate update law: $\dot{\hat{m}}_{\mathrm{f}}(t) = -\Gamma Y_{\mathrm{d}}^T r$

- Closed-loop dynamics

  - Mass parameter estimation error closed-loop dynamics

$$\dot{\tilde{m}}_{\mathrm{f}} = -\Gamma Y_{\mathrm{d}}^T r$$

  - Tracking error closed-loop dynamics

$$\dot{e} = r - \alpha e$$

  - Filter tracking error closed-loop dynamics

$$m_{\mathrm{f}}\dot{r} = Y_{\mathrm{d}}\tilde{m}_{\mathrm{f}} - K_p e - Kr - Cr$$

Lyapunov-based Stability Analysis

- Define a non-negative function

$$V(t) \triangleq \frac{1}{2} m r^T r + \frac{1}{2} e^T K_p e + \frac{1}{2\Gamma} \tilde{m}_{\mathrm{f}}^2$$

- Differentiate with respect to time

$$\dot{V}(t) = r^T m \dot{r} + e^T K_p \dot{e} + \frac{1}{\Gamma} \tilde{m}_{\mathrm{f}} \dot{\tilde{m}}_{\mathrm{f}}$$

- Substitute closed-loop dynamics and utilize skew-symmetry property

$$\dot{V}(t) = -r^T K r - e^T K_p \alpha e$$

- Utilize augmented error variable

$$\dot{V}(t) \leq -\lambda \|\eta\|^2, \qquad \lambda \triangleq \min \left\{ \lambda_{\min} \left\{ K \right\}, \lambda_{\min} \left\{ K_p \alpha \right\} \right\}$$

- Use Barbalat's Lemma to show

$$\lim_{t \to \infty} e(t), \dot{e}(t) = 0$$

Simulation Parameters

Sun-Earth parameters:

$G = 6.671 \times 10^{-11} \frac{\mathrm{m}^3}{\mathrm{kg} \cdot \mathrm{S}^2}$,

$M_{\mathrm{S}} = 1.9891 \times 10^{30}\mathrm{kg}$,

$M_{\mathrm{E}} = 5.974 \times 10^{24}\mathrm{kg}$,

$1\ \mathrm{AU} = 1.496 \times 10^{8}\mathrm{km}$,

$\omega = 2.73774795629 \times 10^{-3} \frac{\mathrm{rad}}{\mathrm{day}}$,

$R_{\mathrm{L}_2} = 1.010033599267463\mathrm{AU}$,

$R_{\mathrm{E}} = \frac{M_{\mathrm{S}}}{M_{\mathrm{E}}+M_{\mathrm{S}}} \times 1\mathrm{AU}$,

$R_{\mathrm{S}} = \frac{M_{\mathrm{E}}}{M_{\mathrm{E}}+M_{\mathrm{S}}} \times 1\mathrm{AU}$

Control and adaptation gains:

$K = \mathrm{diag}\begin{pmatrix} 1, & 1, & 1 \end{pmatrix} \times 1.499 \times 10$,

$\alpha = \mathrm{diag}\begin{pmatrix} 1, & 1, & 1 \end{pmatrix} \times 8.213 \times 10^{-2}$,

$K_p = \mathrm{diag}\begin{pmatrix} 1, & 1, & 1 \end{pmatrix} \times 5.475 \times 10^{3}$,

$\Gamma = 8.888 \times 10^{4}$

Additional parameters:

$$m_{\mathrm{f}} = 1000\mathrm{kg}$$

$$T_{\mathrm{H}} = 1.135225027876099 \times 10^{3}\ \mathrm{day}$$

$$\omega_{\mathrm{Q}} = 6.286301816644046 \times 10^{-5} \frac{1}{\mathrm{day}}$$

- In the simulations, the Halo orbit and the P matrix are approximated using fourier series expansions retaining only 25 terms

Simulation Results: Quasi-periodic Trajectories–I

- Trajectory of the follower spacecraft relative to the nominal Halo orbit using:

$Z_{f_1}(0) = 0, D = 0.0001, \phi = 0, \phi = \frac{\pi}{4}$, and $\phi = \frac{\pi}{2}$

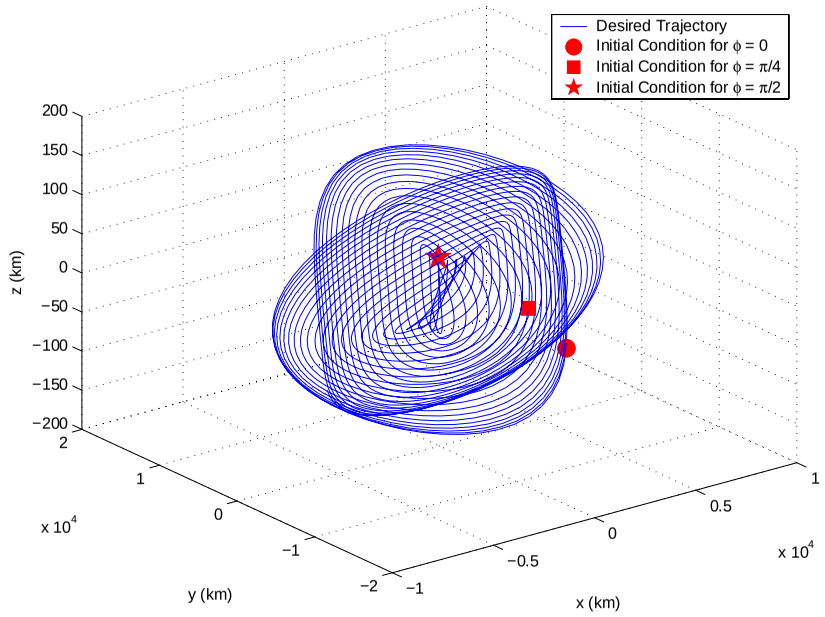

$Z_{f_1}(0) = 0, D = 0.0002, \phi = 0$

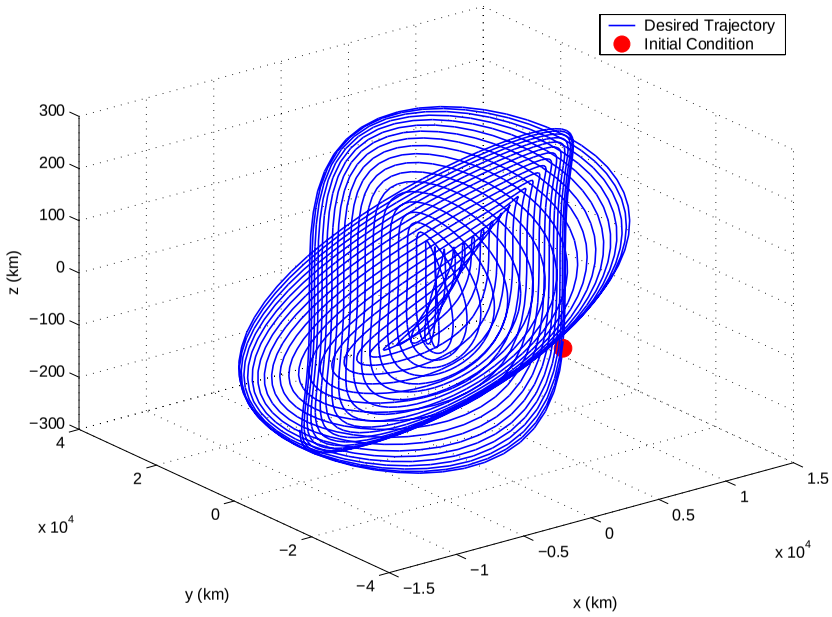

Simulation Results: Quasi-periodic Trajectories–II

- Trajectory of the follower spacecraft relative to the nominal Halo orbit using:

$Z_{f_1}(0) = 0.0001,\ D = 0,\ \phi = 0$

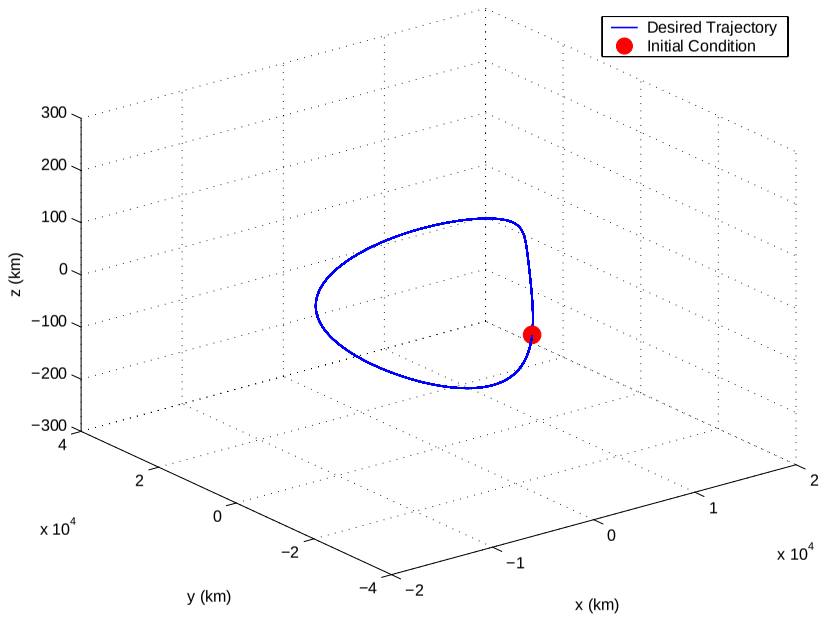

$Z_{f_1}(0) = 0.0001,\ D = 0.0001,\ \phi = 0$

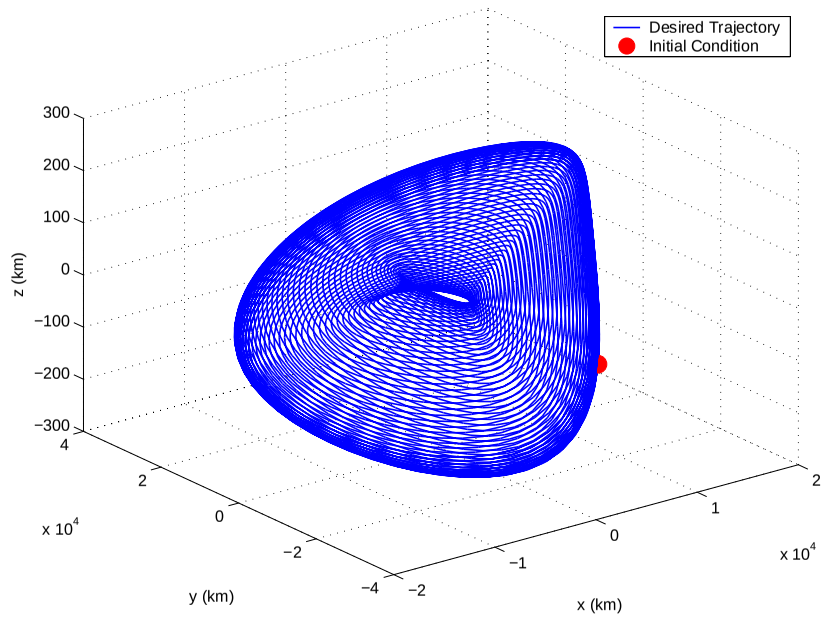

Simulation Results: Adaptive Control Response–I

- q_f relative to Halo orbit:

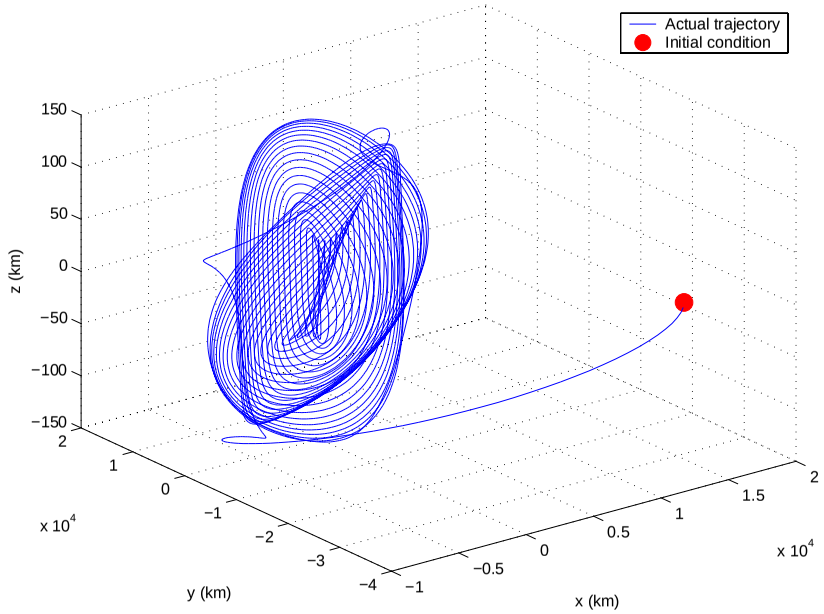

Normal view

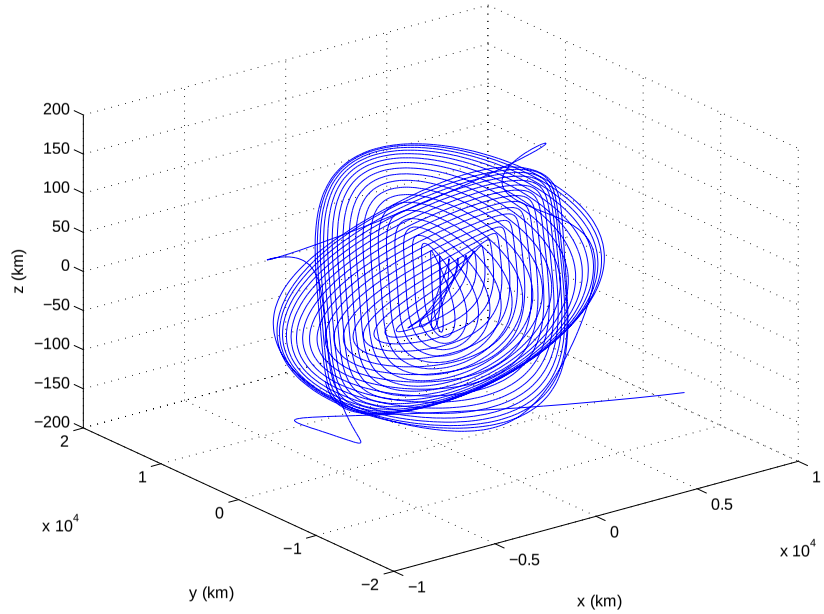

Zoomed in view

Simulation Results: Adaptive Control Response–II

- Tracking error response:

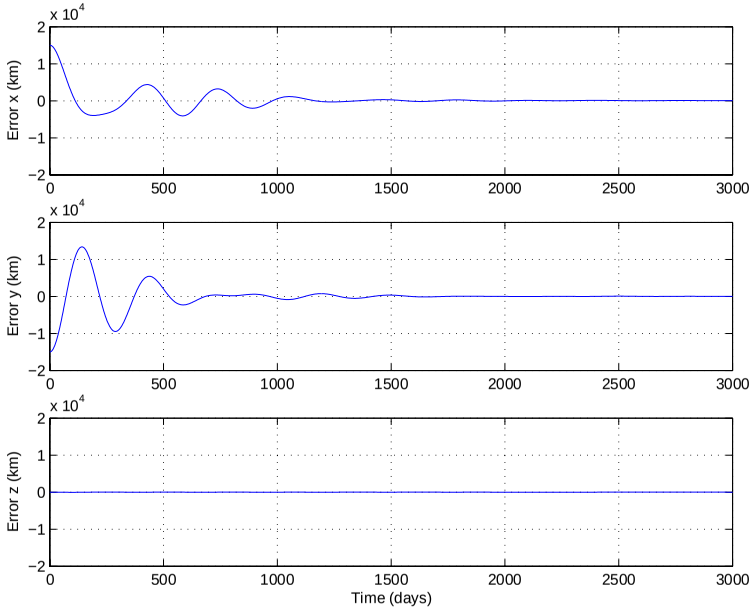

Position tracking error

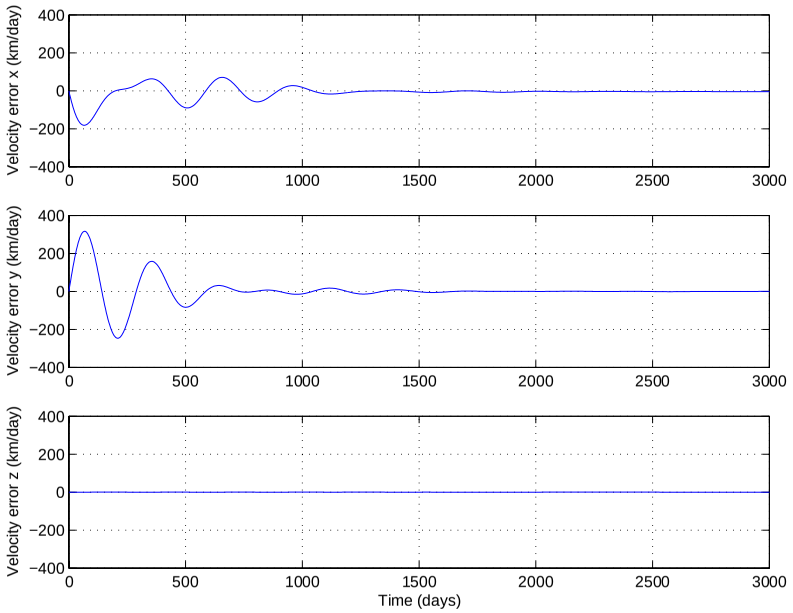

Velocity tracking error

Simulation Results: Adaptive Control Response–III

- Follower spacecraft control and mass parameter estimate response:

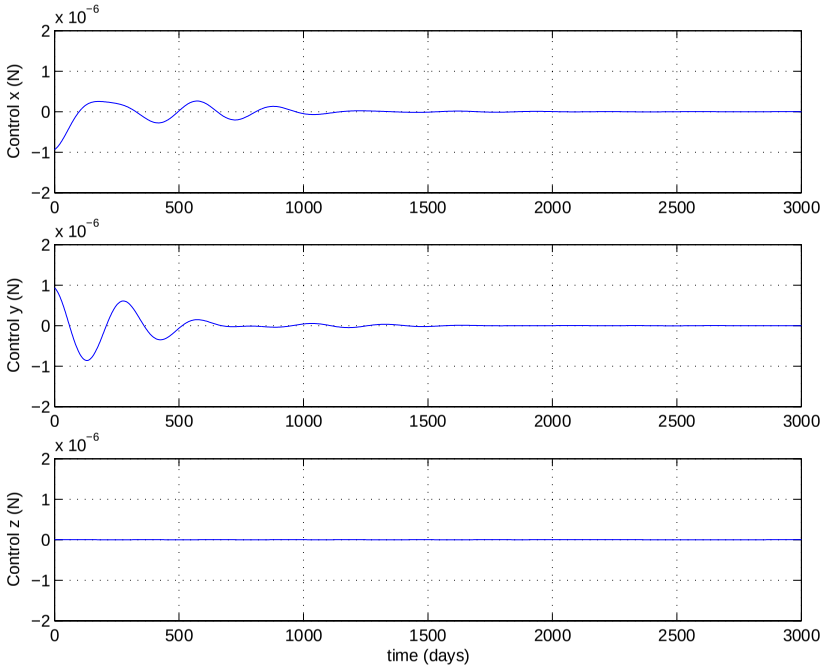

Follower spacecraft control input

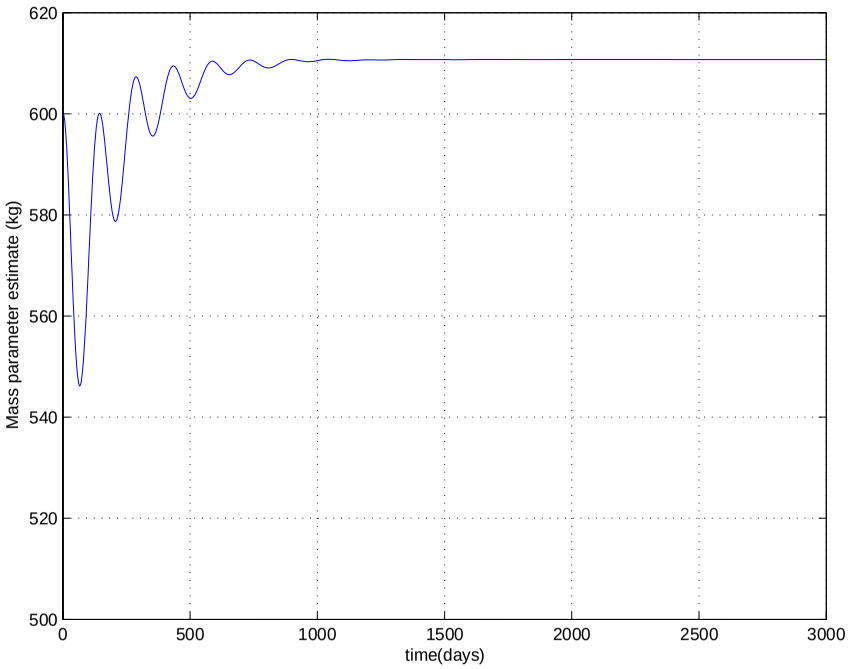

Follower spacecraft mass parameter estimate

Concluding Remarks

- Designed desired quasi-periodic trajectories for the follower spacecraft relative to the leader spacecraft on the Halo orbit
- Size, location, and shape of these trajectories were characterized using a set of parameters
- Illustrative simulations were performed to show these parameter characteristics
- Lyapunov design was used to develop an adaptive full-state feedback controller yielding global, asymptotic convergence of the relative position tracking errors
- Simulation results were presented to show good trajectory tracking